J. Biophoton. **3**, No. 4, 224–233 (2010) / **DOI** 10.1002/jbio.200900107

Journal of BIOPHOTONICS

FULL ARTICLE

Stretching single DNA molecules to demonstrate high-force capabilities of holographic optical tweezers

Arnau Farré[1,2,†], *Astrid van der Horst*[1,3,†], *Gerhard A. Blab*[1], *Benjamin P. B. Downing*[1], *and Nancy R. Forde*[*,1]

[1] Department of Physics, Simon Fraser University, 8888 University Drive, Burnaby, British Columbia, V5A 1S6, Canada
[2] Optical Trapping Lab – Grup de Biofotònica, Departament de Física Aplicada i Òptica, Universitat de Barcelona, Martí i Franquès 1, Barcelona 08028, Spain
[3] Currently at the Department of Physics and Astronomy, VU University, De Boelelaan 1081, 1081 HV Amsterdam, The Netherlands

Received 23 December 2009, revised 28 January 2010, accepted 29 January 2010
Published online 16 February 2010

Key words: holographic optical tweezers, DNA, force measurement

Supporting information for this article is available free of charge under http://dx.doi.org/10.1002/jbio.200900107

The well calibrated force-extension behaviour of single double-stranded DNA molecules was used as a standard to investigate the performance of phase-only holographic optical tweezers at high forces. Specifically, the characteristic overstretch transition at 65 pN was found to appear where expected, demonstrating (1) that holographic optical trap calibration using thermal fluctuation methods is valid to high forces; (2) that the holographic optical traps are harmonic out to >250 nm of 2.1 μm particle displacement; and (3) that temporal modulations in traps induced by the spatial light modulator (SLM) do not affect the ability of optical traps to hold and steer particles against high forces. These studies demonstrate a new high-force capability for holographic optical traps achievable by SLM technologies.

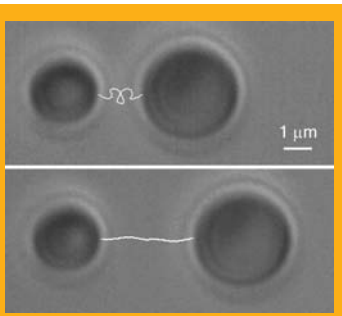

Superposed schematic of a DNA molecule stretched between microspheres held in two holographic optical traps.

1. Introduction

Holographic optical tweezers (HOT) is a technique in which the phase of a trapping laser beam is modulated, for example to generate multiple, steerable trapping foci in a sample chamber. The ability of HOTs to independently manipulate multiple trapped particles in three dimensions in real time has led to their application in a broad range of fields including micropatterning, optical sorting and, more recently, cell biology [1–3]. For the most part, these applications have taken advantage of the ability of optical traps to hold and manipulate particles, but have not made use of their force-measuring capabilities. This is due in large part to uncertainties in the shape of optical traps generated by the discrete phase modulation using spatial light modulators [4, 5], whether the traps can be considered as static when located at

* Corresponding author: e-mail: nforde@sfu.ca, Phone: 778-782-3161, Fax: 778-782-3592
† These authors contributed equally to this work.

© 2010 by WILEY-VCH Verlag GmbH & Co. KGaA, Weinheim

a fixed position within a sample chamber [6, 7], changes in trap stiffness as optical traps are steered within a sample [6, 8], and the maximum forces attainable with this technique [3, 9]. All these questions must be addressed before HOTs find wide acceptance in quantitative force-measuring applications.

Previously, we demonstrated that HOT traps could be positioned with nanometre resolution, and furthermore showed that trap stiffness remained constant within 5% when traps were steered over distances of >20 μm within a sample chamber [6]. These results provided promising evidence that the technique could be used for force-measuring applications [3]. An additional requirement for this application is that HOT traps be capable of exerting high forces on trapped particles and of maintaining particles in the traps as their positions are updated. To date, most applications of this technique have used weak traps for manipulation rather than stiff traps for force measurement. Two recent papers have applied high forces to particles trapped in HOT, estimating that these exceeded 60 pN, however, in both cases, the high forces were calculated by assuming that the trap stiffness obtained at low forces (<2 pN) was valid in the high-force range [3, 9]. The harmonic range of an optical potential depends on many instrument-dependent parameters and on particle size and refractive index. Even for a conventional, non-holographic optical trap, the potential can become anharmonic for relatively small displacements from the trap centre (<100 nm) [10], suggesting that care must be taken when extending trap stiffness calibrations obtained from thermally sampled positions to high forces.

The most common method used to probe the optical potential experienced by a trapped particle is the application of a known drag force on the particle, either by moving the trapping chamber (and entrained fluid) at known speed [8, 9, 11], or by applying known flow speeds to the solution within the chamber [12]. For application to stiff optical traps, the former method requires a stage that can be translated at controlled high speeds, while the second requires controllable flow. Both methods require knowledge of the bead size, which has some uncertainty even for well calibrated commercial samples [13].

We demonstrate here an alternative approach, namely using the well-calibrated force-extension behaviour of DNA, to probe whether the harmonic potential of holographic optical traps extends to forces greater than 65 pN. The elasticity of double-stranded DNA (dsDNA) has been well established from single-molecule stretching experiments [14]. The force-extension curve is highly nonlinear, conforming at low forces to the entropic worm-like chain model of polymer elasticity and exhibiting a plateau at a force of 65 pN. In this so-called overstretch plateau, the molecular contour length increases by 70% as the two strands of DNA melt [15]. Observation of a plateau at 65 pN is a clear signature of a single, torsionally unconstrained dsDNA. The use of DNA as a metrology standard has previously been demonstrated in the low-force regime [16]. Here, we use the overstretch plateau as a force standard to demonstrate the capabilities of HOT for high-force measurements. We compare results of DNA measurements made with our conventional, single-beam optical tweezers instrument to the HOT measurements. We show that our HOT instrument can hold particles in stiff, harmonic traps in the presence of >65 pN of force applied through DNA tension, and that these particles stay trapped in the presence of high tension while trap positions are updated. These results further demonstrate the potential of this technique for high-force measurements.

2. Experimental

2.1 Holographic optical tweezers set-up

Most DNA stretching measurements were conducted using our holographic optical tweezers instrument described previously and shown schematically in Figure 1 [6]. It uses a Holo-Eye HEO 1080P LCOS phase-only spatial light modulator (SLM) to spatially

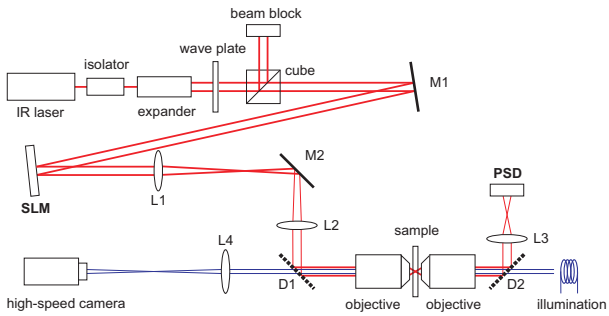

Figure 1 (online color at: www.biophotonics-journal.org) Schematic of the holographic tweezers setup. An infrared laser beam is expanded, after which a half-lambda zero-order wave plate in combination with a polarizing beam splitter cube provides manual control over the power directed to a spatial light modulator (SLM). The SLM modulates the wavefront of the laser beam and the lenses L1 and L2 image the SLM onto the back focal plane of a high-numerical aperture objective lens, which focuses the light to create one or more optical traps. A second identical objective lens captures the light, which is imaged onto a position-sensitive diode (PSD) for trap calibration. The counterpropagating visible light, passing through the dichroic mirrors D1 and D2, is directed to the high-speed camera for particle tracking. See text for details.

© 2010 by WILEY-VCH Verlag GmbH & Co. KGaA, Weinheim

modulate the phase of our 1064 nm trapping laser (Spectra Physics J20-BL-106C), with 2π phase modulation at each pixel. Phase patterns (kinoforms) are generated in LabVIEW using gratings-and-lenses calculations [17] with aberration corrections [18]. The light is focused by a high-numerical-aperture water-immersion objective lens (Olympus UplanApo/IR, 60×, 1.2 NA) into our sample chamber. A position-sensitive photodiode (PSD; OSI Optoelectronics, DL-10) is used for high-bandwidth measurements only to calibrate the trap stiffness of a single trapped particle [6], and is used because it has a much higher bandwidth than our camera. Images of the trapped particles were recorded at 368 frames/second using a high-speed camera (PCO, 1200 HS). Particle positions were determined from these images at high spatial resolution using correlation analysis [6]. In principle, these positions from our high-speed camera could be used to calibrate optical traps, however, for high trap stiffnesses such as used here, camera integration times must be properly taken into account ([19] and A. van der Horst et al., manuscript in preparation).

Figure 2 depicts the experimental geometry in our sample chamber. An end-labelled DNA molecule was stretched between two polystyrene microspheres, which were coated to specifically bind the ends of the DNA (Sections 2.3 and 2.4). Two different sizes of particles were used to distinguish between the labels. One HOT trap was kept stationary while the second was steered to different positions to stretch the DNA. The kinoforms for these positions were precalculated and sent to the SLM as an image stack, so that we reproducibly obtained identical trap separations for the same or different DNA molecules. Trap 1 was located at $(x, y) = (14.3\ \mu m, 8.9\ \mu m)$ with respect to the zero-order spot in the focal plane, while trap 2 was moved stepwise in the range from (17.5 μm, 8.9 μm) to (25.8 μm, 8.9 μm). Trap locations were chosen to avoid ghost traps in the vicinity of the DNA, and to sample more densely the steeper parts of the expected force-extension ($F - z$) curve (35.4 nm steps) while taking larger steps (177 nm) in the flatter parts of the curve. The HOT traps resided at each position for 0.3 seconds (110 image frames on our high-speed camera). At the end of a stretching experiment, when the attachment of the DNA to a particle broke [20], we released the bead in trap 2, after which the trap stiffness for the particle in trap 1, κ_1, was determined from power spectral analysis of its PSD position data [6]. A typical value for these experiments was $\kappa_1 = 250$ pN/μm. In principle, forces could also be measured using trap 2. However, the change in position of this trap for each DNA extension would result in increased uncertainty in particle offset from the trap centre and trap stiffness (Section 3.2), so only trap 1 was used for force measurements.

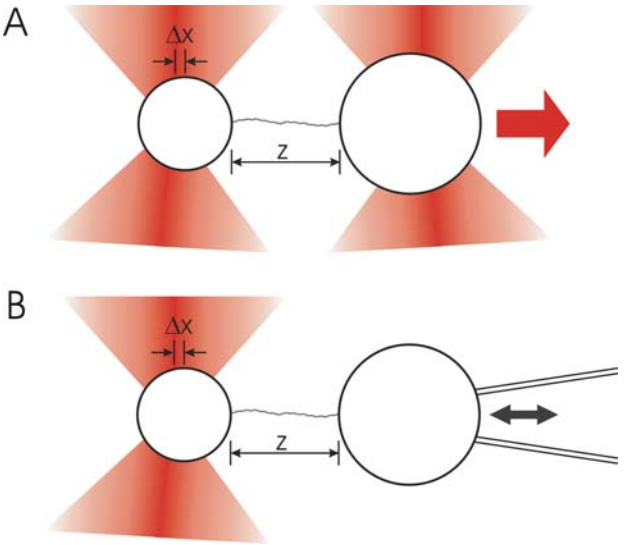

Figure 2 (online color at: www.biophotonics-journal.org) **A.** Schematic of DNA stretching in our HOT instrument. A 2.10-μm-diameter antidigoxigenin-coated polystyrene sphere is trapped in the left, stationary HOT trap (trap 1), while a 3.17-μm-diameter streptavidin-coated polystyrene sphere is displaced stepwise to the right as this HOT trap (trap 2) is steered. An 11.7-kbp-long dsDNA molecule is modified at its ends with biotin and digoxigenin, respectively, which tether the DNA molecule specifically between the microspheres. The force applied to stretch the DNA is determined from the bead displacement from the stationary trap (trap 1), while the extension of the DNA is found from the separation between particles. **B.** Schematic of DNA stretching in our single-beam OT instrument. Here, the optical trap is stationary and the DNA is stretched by moving the micropipette.

2.2 *Single-beam optical tweezers set-up*

We used our separate single-beam optical tweezers instrument, described in more detail previously [21, 22], for control measurements to stretch DNA (Figure 2b). Similar to the HOT setup, it uses water-immersion objectives and a position-sensitive photodiode to produce and calibrate an optical trap, in this case from an 835 nm, 200 mW diode laser. DNA was stretched between an optically trapped bead and a second bead held on the tip of a micropipette by suction. The micropipette was mounted in the sample chamber, which was translated in the plane perpendicular to the optical axis by a nanometre-precision two-axis piezoelectric stage (Mad City Labs, Nano H-50). DNA stretching experiments were performed using the same polystyrene microspheres and DNA samples as in the HOT experiments. Images of the particles were recorded and saved at 10 Hz using a CCD camera (Flea, Point

© 2010 by WILEY-VCH Verlag GmbH & Co. KGaA, Weinheim

Grey Research) and their positions were determined by correlation analysis.

2.3 DNA preparation and labelling

Double-stranded DNA molecules used in our experiments were obtained by digestion of plasmid pPIA2-6 [23] with restriction endonucleases EagI (New England Biolabs) and EcoRI (Invitrogen). The purified 11.7 kilobasepair (kbp) fragment was labelled using Klenow exo- DNA polymerase (Fermentas) and a mixture of dATP, dGTP, biotin-dCTP (Invitrogen) and digoxigenin-dUTP (Roche), each at 33 μM, resulting in dsDNA with two biotin groups at one end and two digoxigenin groups at the other.

2.4 Bead preparation and testing

Streptavidin (Molecular Probes) was crosslinked to carboxyl functionalized 3.17-μm diameter polystyrene microspheres (Spherotech) using EDC (Fluka Analytical). 2.10 μm diameter polystyrene microspheres, covalently coated with protein G (Spherotech), were allowed to react with anti-digoxigenin (Roche), whose Fc region binds to protein G. This interaction was then stabilized by crosslinking with DMP (Sigma-Aldrich). Before a stretching experiment, DNA was incubated for an hour at room temperature with the anti-digoxigenin beads, letting the antibody-antigen interaction coat the beads in DNA. The DNA concentration was approximately 0.1 nM during incubation, with a ratio of no more than 100 DNA molecules per bead. The beads were then incubated with 10 mg/ml BSA for 20 minutes to block non-specific binding, and finally washed to remove unbound DNA and BSA.

We have developed an assay for DNA binding to our anti-digoxigenin-coated microspheres, and tested it on a 2.1 kbp DNA fragment labelled using a protocol similar to that described in Section 2.3. Anti-digoxigenin beads and labelled DNA were incubated as described above. Unbound DNA was removed through repeated washing steps. The beads were then incubated for one hour on a mixer at room temperature with streptavidin alkaline phosphatase (Promega), which can bind to biotin on the free end of the DNA molecules. Free streptavidin alkaline phosphatase was washed away. The beads were then incubated with pNPP (Sigma-Aldrich), whose hydrolysis is catalysed by alkaline phosphatase to produce a yellow substrate with a strong absorbance peak at 405 nm. By ensuring pNPP was in excess and the incubation time was sufficiently short, the absorbance at 405 nm was proportional to the quantity of streptavidin alkaline phosphatase present, and so to the number of biotinylated DNA molecules. We normalized the optical density at 405 nm by the bead concentration to obtain a value proportional to the average number of DNA molecules bound per bead. Bead concentration was determined for each sample by measuring the intensity of 532 nm laser light it scattered at 90°, and comparing this to a calibration curve produced from samples of known concentration.

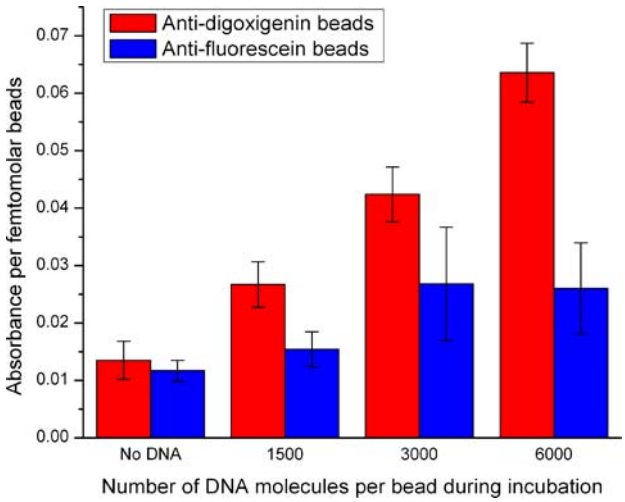

Figure 3 (online color at: www.biophotonics-journal.org) Results of pNPP quantification of DNA binding to beads. Beads were incubated with labelled DNA at the indicated ratios, then quantified. DNA bound specifically to anti-digoxigenin coated beads and non-specifically to the anti-fluorescein coated control beads. The finite signal when no DNA was present indicated non-specific binding of streptavidin-alkaline phosphatase to the beads. Error bars show the standard deviation of 3 separate trials.

By using this assay, we confirmed that digoxigenin-labelled DNA was successfully bound to the anti-digoxigenin beads and had accessible biotins (Figure 3). Signal increased with DNA concentration, and was greater for specifically bound DNA (incubated with anti-digoxigenin beads) compared with non-specifically adsorbed DNA (incubated with anti-fluorescein coated beads). Due to the significant level of background signal in the absence of DNA, the assay works best for large numbers of bound DNA molecules (here, approximately 10 times the number per bead used in the single-molecule experiments), so is best suited to experiments testing whether or not bead and DNA labelling is effective.

2.5 Force-extension measurements of DNA

Experiments were performed in the middle of home-made multistream flow cells that consisted of two

© 2010 by WILEY-VCH Verlag GmbH & Co. KGaA, Weinheim

microscope cover slips sandwiching a fluid channel created by excising a Y-shaped physical channel from the centre of a Nescofilm spacer (NESCO; chamber volume 10–20 μl). Holes drilled in one of the coverslips permitted fluid flow through two inlets and an outlet; the two inlet channels allowed us to use streptavidin and DNA-coated anti-digoxigenin microspheres simultaneously without mixing [24]. Before every experiment, both the chamber and the beads were washed with 10 mg/ml bovine serum albumin (BSA) to prevent non-specific interactions between the beads and glass surfaces. Experiments were conducted in a buffer solution (150 mM NaCl, 10 mM Tris and 1 mM EDTA, pH 8.0) in which the overstretch transition of dsDNA is expected to occur at 65 pN [25].

At the beginning of an experiment, the flow cell was positioned such that the traps were close to the interface between streams and only one type of beads was present in the field of view. After trapping one of the microspheres with a holographic trap, the chamber was moved up-/downwards, past the interface, to trap the other type of bead in a second holographic trap. Finally, the flow was stopped and the sample chamber repositioned so that the two trapped beads were in a region free of other beads. The two trapped microspheres were brought in proximity to enable the formation of the biotin-streptavidin interaction. (The 2- and 3-μm particles used in these experiments facilitated close approach of the two bead surfaces while maintaining a relatively large separation between the traps.) Tethers were detected by the tension-induced displacement of particles from the trap centres. In the HOT instrument, many tethers lasted only tens of seconds, much shorter lifetimes than in the single-beam optical tweezers instrument. This lifetime shortening was due to the higher power 1064 nm laser and could be improved by adding an oxygen scavenging system (PCA/PCD) to the sample [20].

Tethered DNA molecules were stretched stepwise using predetermined kinoforms, as described above. Camera images were analysed to obtain the positions of the particles and the offset of the particle from trap 1 as a function of time. Unless otherwise specified, the end-to-end extension of DNA, $z(t)$, was determined in each image using the positions of each particle relative to its initial position $(x_1(t), x_2(t))$, plus a fixed offset x_0: $z(t) = x_2(t) - x_1(t) + x_0$. The force applied to the bead in trap 1 (equal in magnitude to the tension in the DNA) was determined from $F_1(t) = -\kappa_1 x_1(t) + F_0$. The force and displacement offsets, constant for a given tether, are necessary because our correlation algorithm provides the position of each particle relative to its position in an initial reference template image, not an absolute position measurement [6].

Force-extension curves of DNA molecules were fit with the inextensible worm-like chain (WLC) model of entropic elasticity [26, 27]:

$$F(z) = \frac{k_B T}{L_p}\left[\frac{1}{4\left(1-\frac{z}{L_c}\right)^2} + \frac{z}{L_c} - \frac{1}{4}\right]. \quad (1)$$

L_c is the contour length of the DNA (in our case 3.96 μm), L_p is its persistence length, k_B is Boltzmann's constant and T is the absolute temperature. L_p and the offsets x_0 and F_0 are the fitting parameters used for each experimental force-extension curve. There is a strong interdependence among these three parameters, particularly evident when fitting a limited number of F-z data points as from our HOT measurements. Thus, an estimate of x_0 and F_0 was first obtained by setting $L_p = 53$ nm; using these values as initial guesses for a least-squares fit, x_0, F_0 and L_p were allowed to vary to best fit the available data. DNA's force-extension behaviour is known to deviate from the inextensible WLC model at high forces [28], and so fits reported here were performed to data points below 5 pN.

For determinations of the residuals between the experimental HOT $F - z$ data and a WLC fit, only x_0 and F_0 were allowed to vary in fitting each curve, while $L_c = 3.96$ μm and $L_p = 45$ nm were held fixed. (This value of L_p was used for consistency with the average value found for this sequence of DNA in our single-beam optical tweezers instrument.) The point of this analysis was to quantify observed modulations, and thus it was important to compare the measurements to the same model, even if this did not represent the best fit for each curve that would have been obtained by allowing L_p to vary.

3. Results and discussion

3.1 Stretching DNA to high force

Supplementary Movie 1 shows a DNA stretching experiment with three stretches and relaxations. Still images from such an experiment are shown as the figure in the abstract to this article (with a schematic of a tethered DNA molecule superposed for illustrative purposes). Figure 4 shows a plot of each bead's position as a function of time as a DNA molecule is stretched, with the tether breaking at the end of this experiment. The regions of different slope are due to the difference in step sizes chosen for sampling different regions of the force-extension curve. As trap 2 is steered and the DNA stretched, the gradual displacement of particle 1 from the stationary trap is

© 2010 by WILEY-VCH Verlag GmbH & Co. KGaA, Weinheim

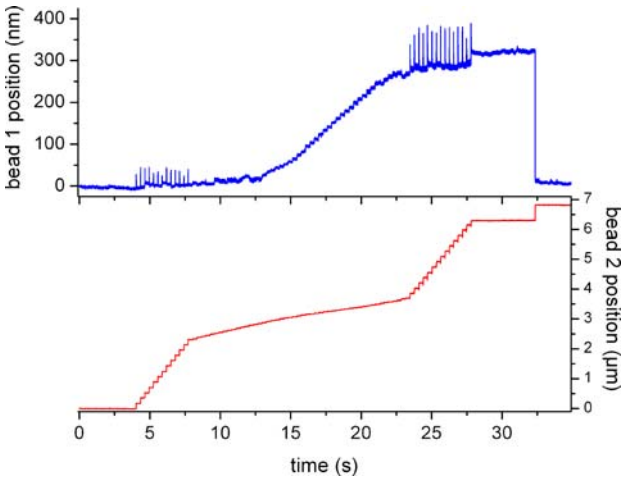

Figure 4 (online color at: www.biophotonics-journal.org) Bead positions vs. time as obtained from high-speed camera images for the bead in trap 1 (top) and the bead in trap 2 (bottom), from a representative DNA stretching experiment. The different position scales arise because trap 2 is being steered.

clear (10–22 s), indicating increasing applied force, as is its approximately constant displacement during the overstretch transition (22–30 s). An additional feature is also apparent in these data: beads displace substantially during the update of a trap position (seen by the spikes in the trace of particle 1; particle 2 experiences displacements of similar magnitude, not seen because of the scaling in Figure 4). This effect has been noted previously for HOT traps [29] and is discussed more, below. In our experiments, particle excursions were greater for larger steps of trap 2, so could be minimized by using smaller step sizes, if desired. To ensure these dynamics were excluded from our analysis, the average particle positions for each kinoform were determined using only the central 60% of the data at each extension (66 data points).

The average positions of the trapped particles, as determined from video tracking, were used to determine the end-to-end extension of the DNA, z, and the force, F, required to attain this extension, as described in the Methods Section. A representative force-extension curve of DNA, recorded in our HOT instrument, is shown in Figure 5. This shows the expected WLC response at low forces, followed by the characteristic overstretch transition at 65 pN. The appearance of the plateau at 65 pN demonstrates that the calibrated trap stiffness from the power spectrum of thermally induced motion is valid to forces of at least 65 pN. For these experiments with a trap stiffness of $\kappa_1 = 250$ pN/μm, our results demonstrate that 2.10-μm-diameter particles in stiff HOT traps experience a harmonic potential out to displacements of at least 260 nm.

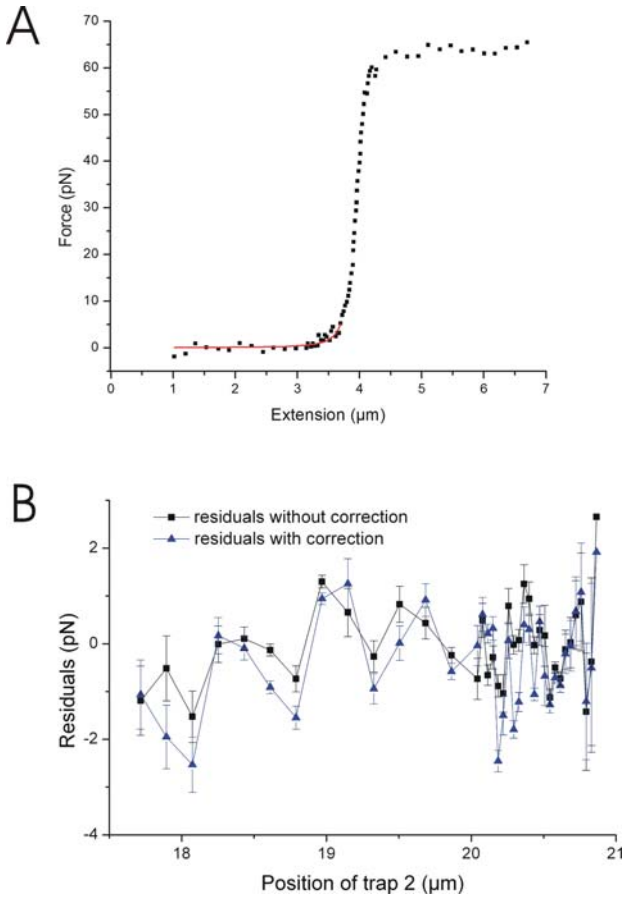

Figure 5 (online color at: www.biophotonics-journal.org) **A.** Representative force-extension curve of DNA, showing characteristic overstretch transition at 65 pN. Overlaid on the black data points is a WLC fit with $L_p = 45$ nm. The small number of data points involved in the fit below 5 pN results in large uncertainties of fitting parameters. If more information about this low-force region were desired, trap 2 could be stepped in smaller increments. **B.** Force residuals from WLC fits to F-z data from 4 different molecules (7 curves) showing systematic deviation from expected values (black squares). The positions here correspond to the region <5 pN in plot a. Data points represent the mean values and error bars the standard errors of the means. Lines are a guide to the eye. Using a corrected position of trap 1, determined for each position of trap 2, the force residuals are altered but still display systematic modulations (blue triangles).

The spikes in Figure 4 correspond to updates of the position of trap 2. It is remarkable that the trapped particles are not lost during this refreshing of the SLM, particularly because of the significant tension in the DNA. Previous work showed that HOT traps can be repositioned in step sizes of a bead radius without losing the trapped particle, even in the presence of external flow [29]. The maximal forces exerted in that work were approximately 2 pN. Here, our results show that the trap position

© 2010 by WILEY-VCH Verlag GmbH & Co. KGaA, Weinheim

can be changed in 177 nm steps and, for our system, the particles are retained in the traps even in the presence of 65 pN of force exerted through the DNA. Additionally, these results demonstrate that the 300 Hz trap modulations introduced by our SLM [6, 7] do not affect the ability of the HOT traps to maintain particles in the presence of high external force.

3.2 *Apparent force modulations*

Force-extension curves measured for DNA in our HOT instrument exhibit apparent force modulations (Figure 5), most clearly seen in the flatter portions of the curves. These appear to be systematic, as seen by the non-zero average force residuals between WLC fits and measured $F - z$ data. The modulations are not due to the DNA or beads used in these experiments. Figure 6 shows an example of a force-extension curve recorded for DNA from the same sample, immobilized using beads from the same preparation, stretched in our single-beam optical tweezers instrument. It is clear that this measurement shows the expected WLC behaviour at low forces, and furthermore, exhibits the overstretch plateau at 65 pN, as expected. Thus, the modulations observed in the HOT measurements are specific to that instrument.

We sought to account for these small, yet systematic, modulations by examining our assumptions of a stationary trap 1 and of constant trap 1 stiffness.

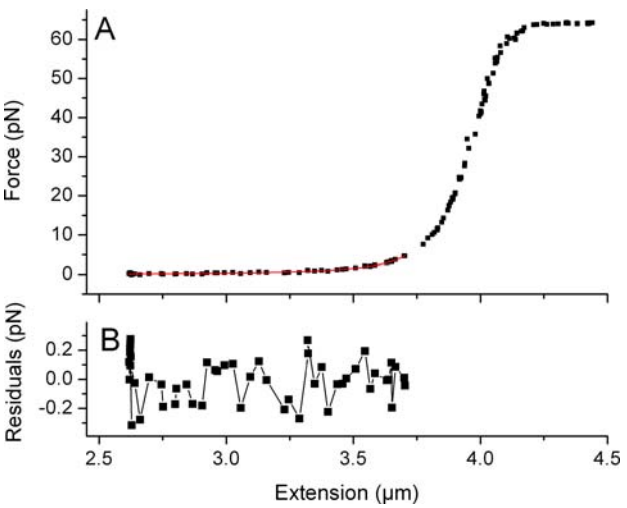

Figure 6 (online color at: www.biophotonics-journal.org) **A.** Representative force-extension curve of DNA recorded in our single-beam optical tweezers instrument, showing the WLC fit to the data ($L_p = 48$ nm). **B.** Residuals of force from this WLC fit, which are much smaller than for the HOT stretching data. Lines are a guide to the eye.

If either of these values changed during a stretching experiment, we would miscalculate the true force, since forces are determined from $F_1(t) = -\kappa_1 \, \Delta x_1(t)$.

Close examination of Figure 4 reveals discontinuous changes in the position of trap 1 throughout the experiment, an effect particularly perceptible in the flatter portions of the curve. To determine the extent of this movement, we performed separate experiments using the same kinoforms, in which a 2.10 μm particle was trapped in trap 1. An "empty" trap 2 was then stepped alternately between its maximum separation from trap 1 and intermediate positions, to minimize contributions of drift to these measurements [6], and the mean position of the bead in trap 1 at each position of trap 2 was determined from image analysis. As seen in Figure 7, deviations of these mean positions from the overall average position are small (<6 nm) but reproducible. They are apparent in both x and y directions, although the deviations in the direction perpendicular to trap steering are considerably smaller than in the parallel direction. Using the "corrected" trap 1 positions for each kinoforms (Figure 7), we recalculated the forces in our DNA measurements. While slightly changing the F-z curve, a systematic deviation in force residuals of the same order as before correction remained (Figure 5b).

We also investigated whether the apparent modulations in force arose from significant changes in trap stiffness in trap 1 as trap 2 was steered. Based on our previous work, this was not expected, but the

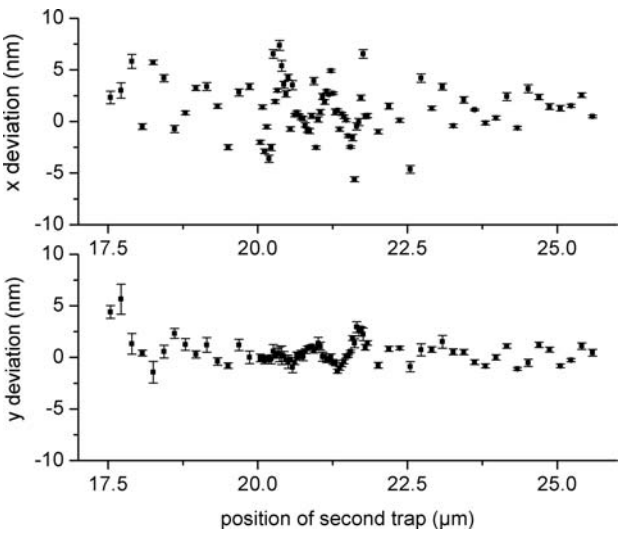

Figure 7 The position of the particle in trap 1 versus the x position of trap 2. Plotted are the deviations of the mean positions from the overall average position for particle 1 in both x (top) and y (bottom) directions. The error bars indicate the standard deviation ($N = 8$). Systematic deviations in both directions from the mean position are observed, even though trap 2 is steered only in the x direction.

© 2010 by WILEY-VCH Verlag GmbH & Co. KGaA, Weinheim

positions used here brought the particles closer to each other than we had previously studied [6]. We performed power spectrum measurements of a 2.10 μm particle held in trap 1 with positions of trap 2 corresponding to the maximum and minimum positions of trap 1 measured in Figure 7 (20.4 μm and 21.6 μm, respectively). The calibrated stiffness values differed by only 2% (data not shown), an insignificant change.

It is possible that the modulations arise from out-of-plane motion of particle 1: the correlation algorithm we use is designed to track particle positions in the (x, y) plane only. Out-of-plane motion, along the optic axis, could result in perceived motion in the (x, y) plane, resulting in a measured apparent displacement of the trapped particle. In these measurements, with DNA stretched in the x direction, out-of-plane motion would arise from the shift of the traps along the optic axis. This should be accounted for by correcting the position of trap 1 (Figure 7). Furthermore, if the DNA were being stretched increasingly out of the (x, y) plane, the z-offset of a bead should change monotonically with increasing trap separation, not in an oscillatory fashion. This monotonic axial displacement was observed for some tethers, as seen in Supplementary Movie 1, though was generally most apparent immediately before losing the particle from the trap.

The most likely source of the observed modulations is interference between the two holographic traps [A. Farré et al., manuscript in preparation]. Work with two non-holographic optical traps found that even with orthogonally polarized beams, a 2% cross-talk between beams existed, giving rise to changes in intensity and light distribution within the two traps [13]. This resulted in modulations in trap positions on the order of 1 nm for traps separated by >500 nm, which increased to 5 nm as the traps approached closer. Presumably, such interference effects would be more evident with both traps having the same polarization, as in our case of phase-modulated HOT traps created with the same SLM. It is therefore somewhat surprising, although pleasantly so, that the modulations we observe here are only on the order of ~6 nm, and were only on the order of <2 nm for previous work with traps separated by distances of ~9 μm [6].

4. Conclusions

These studies have conclusively shown that calibrated high forces (>65 pN) are attainable with SLM-based holographic optical tweezers. In our setup, this demonstrates that HOT traps are harmonic out to displacements of >250 nm for 2.10 μm trapped particles. Furthermore, even though high forces are exerted on the trapped particles through DNA tension, particles are not lost from the HOT traps as trapping kinoforms are updated on the SLM.

The maximal laser power, and hence trap stiffness, are limited by the damage threshold of the SLM. The trap stiffness ($\kappa \sim 250$ pN/μm) we have used here is a factor of three higher than previous maximum stiffnesses reported for HOT traps [3, 6]. In principle, for single-molecule stretching experiments, two traps of different stiffness could be created, providing one trap of higher stiffness than we have used (and thereby increasing the maximum force obtainable within the harmonic region), but this was unnecessary for the present work.

We observed small (<2 pN) but systematic modulations in apparent force applied to the DNA as a function of particle separation. This is likely due to optical interference between holographic traps, which can result in changes of the equilibrium position of particles by ~5 nm, but is not manifest as changes in trap stiffness. While these modulations are undesired, they are small when compared with force and length scales for measurements of soft biomaterials [30] and thus should not prove problematic for application of this technique to quantitative high-force measurements.

Acknowledgements We thank Andrew Wieczorek for assistance developing the pNPP assay. This work is supported by a Discovery Grant from the Natural Sciences and Engineering Research Council of Canada (NSERC), funding from the Canada Foundation for Innovation (CFI) and from the Human Frontier Science Program (HFSP). AF is sponsored by a doctoral research fellowship from the Generalitat de Catalunya (grant FI). BPBD thanks NSERC and the Michael Smith Foundation for Health Research (MSFHR) for fellowship support. NRF is a Cottrell Scholar of the Research Corporation and an MSFHR Scholar.

Arnau Farré obtained his B.Sc. in Physics from the Universitat de Barcelona (Spain) in 2007 and his M.Sc. in Biophysics from the same university in 2008. He is currently a Ph.D. student in the field of optical tweezers and biological applications in the Optical Trapping Lab – Grup de Biofotònica at the Universitat de Barcelona (UB). During the first semester of 2009, Mr. Farré worked in the Department of Physics at Simon Fraser University, where he carried out the present work.

© 2010 by WILEY-VCH Verlag GmbH & Co. KGaA, Weinheim

Astrid van der Horst did her Ph.D. research on optical trapping both in the Bio-Assembly and Organization group of Marileen Dogterom at the FOM-Institute for Atomic and Molecular Physics (AMOLF) in Amsterdam and in the Soft Condensed Matter group of Alfons van Blaaderen at Utrecht University, the Netherlands. She was a postdoctoral researcher at Simon Fraser University from 2006–2009 and currently holds a 3-year postdoctoral fellowship from the Foundation for Fundamental Research on Matter (FOM) at the VU University in Amsterdam.

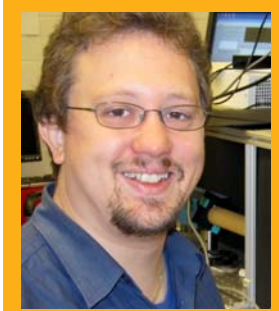

Gerhard Blab obtained his Dipl.-Ing. in Biophysics from the Johannes Kepler University in Linz, Austria and his Ph.D. in Physics from Leiden University in the Netherlands. He currently works as a postdoctoral researcher at Simon Fraser University.

Benjamin Downing obtained his B.Sc. in Physics from Dalhousie University. He is currently an M.Sc. student in the Department of Physics at Simon Fraser University.

Nancy Forde obtained her B.Sc. in Chemical Physics from the University of Toronto, her Ph.D. in Chemistry from the University of Chicago, and was a postdoctoral researcher and HHMI associate with Carlos Bustamante at UC Berkeley. She has been a faculty member in the Department of Physics at Simon Fraser University since 2004, where she leads an interdisciplinary biophysics research group.

References

[1] K. Dholakia, P. Reece, and M. Gu, Chem. Soc. Rev. **37**, 42 (2008).
[2] D. G. Grier, Nature **424**, 810 (2003).
[3] C. O. Mejean, A. W. Schaefer, E. A. Millman, P. Forscher, and E. R. Dufresne, Opt. Express **17**, 6209 (2009).
[4] G. Sinclair, J. Leach, P. Jordan, G. Gibson, E. Yao, Z. Laczik, M. Padgett, and J. Courtial, Opt. Express **12**, 1665 (2004).
[5] J. Xia and H. Yin, Opt. Eng. **48**, 020502 (2009).
[6] A. van der Horst and N. R. Forde, Opt. Express **16**, 20987 (2008).
[7] A. van der Horst, B. P. B. Downing, and N. R. Forde, in Optical Trapping Applications (Optical Society of America, Washington, DC, 2009), p. OMB3.
[8] F. Belloni, S. Monneret, F. Monduc, and M. Scordia, Opt. Express **16**, 9011 (2008).
[9] L. Ikin, D. M. Carberry, G. M. Gibson, M. J. Padgett, and M. J. Miles, New J. Phys., 023012 (2009).
[10] W. J. Greenleaf, M. T. Woodside, E. A. Abbondanzieri, and S. M. Block, Phys. Rev. Lett. **95**, 208102 (2005).
[11] K. C. Neuman and S. M. Block, Rev. Sci. Instrum. **75**, 2787 (2004).
[12] G. J. L. Wuite, R. J. Davenport, A. Rappaport, and C. Bustamante, Biophys. J. **79**, 1155 (2000).
[13] C. Bustamante, Y. R. Chemla, and J. R. Moffitt, Cold Spring Harbor Protocols **2009**, doi:10.1101/pdb.ip73 (2009).
[14] C. Bustamante, Z. Bryant, and S. B. Smith, Nature **421**, 423 (2003).
[15] J. van Mameren, P. Gross, G. Farge, P. Hooijman, M. Modesti, M. Falkenberg, G. J. L. Wuite, and E. J. G. Peterman, Proc. Nat. Acad. Sci. USA **106**, 18231 (2009).
[16] J. P. Rickgauer, D. N. Fuller, and D. E. Smith, Biophys. J. **91**, 4253 (2006).
[17] D. R. Burnham and D. McGloin, Opt. Express **14**, 4175 (2006).
[18] K. D. Wulff, D. G. Cole, R. L. Clark, R. DiLeonardo, J. Leach, J. Cooper, G. Gibson, and M. J. Padgett, Opt. Express **14**, 4169 (2006).
[19] W. P. Wong and K. Halvorsen, Opt. Express **14**, 12517 (2006).
[20] M. P. Landry, P. M. McCall, Z. Qi, and Y. R. Chemla, Biophys. J. **97**, 2128 (2009).
[21] Y. Deng, J. Bechhoefer, and N. R. Forde, J. Opt. A: Pure. Appl. Opt. **8**, S256 (2007).
[22] B. P. B. Downing, A. van der Horst, M. Miao, F. W. Keeley, and N. R. Forde, in Optical Trapping Applications (Optical Society of America, Washington, DC, 2009), p. OTuA3.
[23] R. J. Davenport, G. J. L. Wuite, R. Landick, and C. Bustamante, Science **287**, 2497 (2000).
[24] L. R. Brewer and P. R. Bianco, Nat. Meth. **5**, 517 (2008).
[25] S. B. Smith, Y. J. Cui, and C. Bustamante, Science **271**, 795 (1996).

© 2010 by WILEY-VCH Verlag GmbH & Co. KGaA, Weinheim

[26] C. Bustamante, J. F. Marko, E. D. Siggia, and S. Smith, Science **265**, 1599 (1994).
[27] J. F. Marko and E. D. Siggia, Macromol. **28**, 8759 (1995).
[28] C. Bouchiat, M. D. Wang, J. F. Allemand, T. Strick, S. M. Block, and V. Croquette, Biophys. J. **76**, 409 (1999).
[29] E. Eriksson, S. Keen, J. Leach, M. Goksör, and M. J. Padgett, Opt. Express **15**, 18268 (2007).
[30] G. Lenormand, S. Henon, A. Richert, J. Simeon, and F. Gallet, Biophys. J. **81**, 43 (2001).

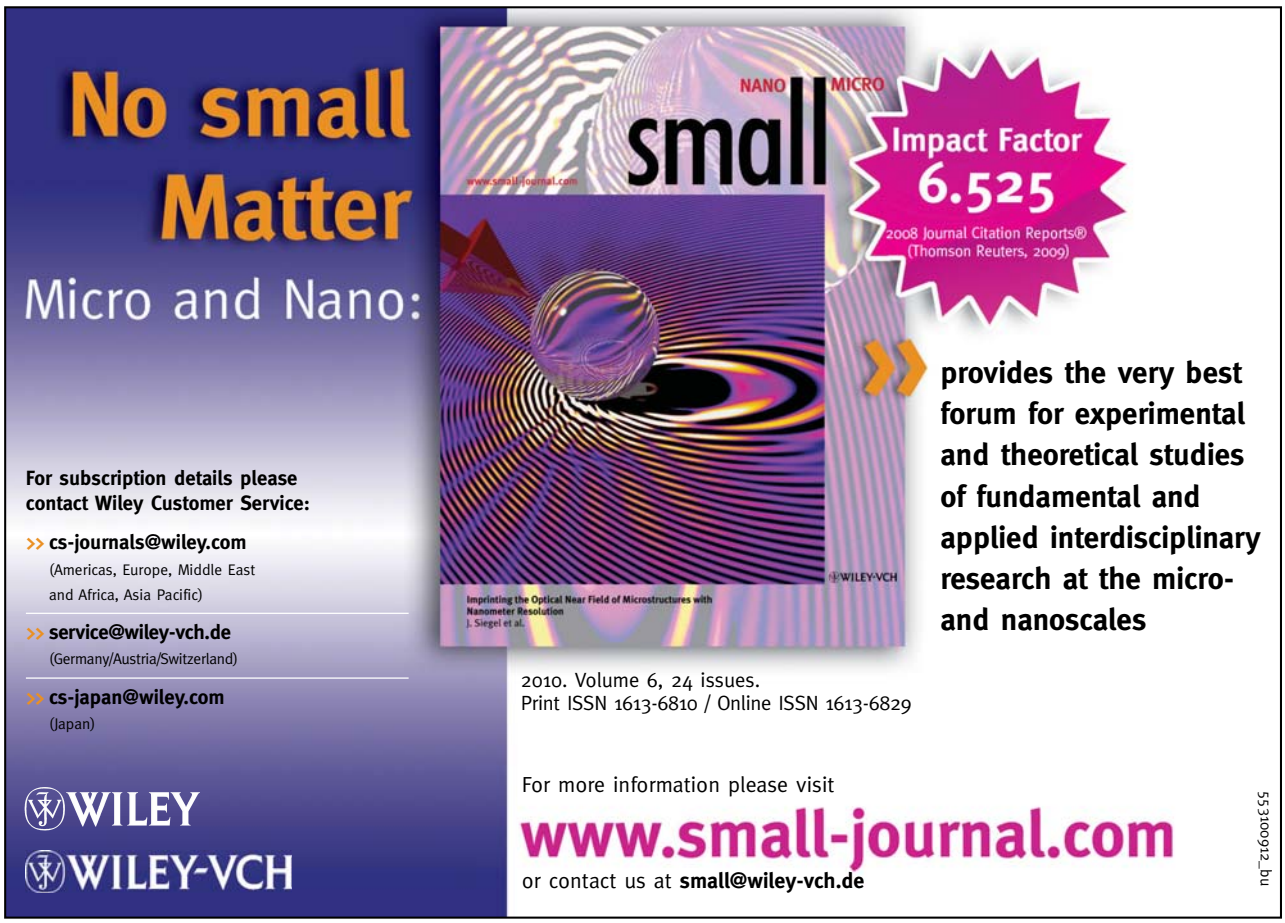

© 2010 by WILEY-VCH Verlag GmbH & Co. KGaA, Weinheim